Investigation into double yield points in polyethylene

N. W. Brooks, R. A. Duckett* and I. M. Ward
IRC in Polymer Science and Technology, University of Leeds, Leeds LS2 9JT, UK
(Received 28 May 1991; accepted 6 August 1991)

The effects of branching on the yield of polyethylene have been investigated using three polyethylene samples with differing degrees of short-chain branching. The experimental results have shown the existence of double yield points for all three samples. The double yield points are evident from the shapes of the stress–strain curves obtained for the three samples over a range of temperatures. Measurement of the residual strains of the samples as a function of the level of maximum strain applied under constant elongation rate test show that the first yield point marks the onset of 'plastic strains' which are slowly recoverable at least in part. Deformation beyond the second yield point is effectively irrecoverable and is associated with a sharp necking of the samples. The yield points are interpreted mechanically as the yield of two dashpots and the model used to describe the yield is of two non-linear Maxwell elements in parallel. Transient dip experiments have been used to separate the stress–strain curves of the individual arms and these confirm that the two arms do yield at different strains.

(Keywords: polyethylene; yield; chain branching)

INTRODUCTION

This paper describes a detailed investigation of the yield behaviour of three very different polyethylene polymers, which vary with respect to both molecular weight and short-chain branch content. Initially two fundamental questions had to be addressed, namely, what is yield and how do we measure it quantitatively?

The measurement of a yield point in polymers is conventionally accepted as being the point where the force–elongation curve shows a local maximum. The stress and strain values associated with this point are the yield stress and yield strain values for the material under the given conditions. For samples which initially deform homogeneously this maximum occurs as a result of the internal plastic strain rate of the material increasing to a point where it becomes equal to the applied strain rate. In some instances a maximum in force also relates to the onset of necking, where strain hardening of the necked materials is not sufficient to counteract the reduction of the cross-sectional area, leading to a reduction in load.

For the polyethylene samples investigated this maximum becomes less defined as the testing temperature is increased or the strain rate is decreased. The maximum disappears at a given temperature and strain rate and the material starts to display a stress–strain curve of the type shown in *Figure 1*. The temperature at which the local maximum disappears is lowest for the most branched material and highest for the unbranched, high density material.

The curve shown in *Figure 1* obviously does not show a conventional yield point so we must use a different way of measuring the yield point. It is common to use two other methods to measure the yield point for this type of curve. The first is to use an offset yield point and the second is to use a method of intersecting lines from the initial modulus and the almost linear region past the yield point. The method of intersecting lines is difficult to justify, and so is the offset yield point.

It was therefore decided to investigate the shape of these curves in more detail. It was decided to model the curves mathematically and then, combining this model with the Considère construction, to predict the point where there is a local force maximum in the material.

The mathematical modelling of the curve was based on ideas proposed by Brereton *et al.*[1] for non-linear viscoelastic materials, using an equation of the form:

$$a\sigma + b\varepsilon + c\sigma\varepsilon = 0$$

here a, b and c are, in general, time-dependent material response functions which model the non-linear viscoelastic behaviour and are affected by the thermal and mechanical history of the material. If it is assumed initially that these functions are time independent then the above equation can be rewritten to give the following equation for the true stress:

$$\sigma = \frac{E\varepsilon}{1 + \beta\varepsilon} \tag{1}$$

where σ and ε have their usual meaning, E is the initial modulus and β is a dimensionless constant which provides a feedback term. In a preliminary analysis both E and β can be considered as parameters which are temperature and strain rate dependent.

At small strains, $\beta\varepsilon \ll 1$, and so equation (1) approximates to a simple Hookean spring. At higher strains the feedback terms become more important. As $\varepsilon \to \infty$, $\beta\varepsilon \gg 1$, and the stress tends to a critical value,

*To whom correspondence should be addressed

0032-3861/92/091872-09

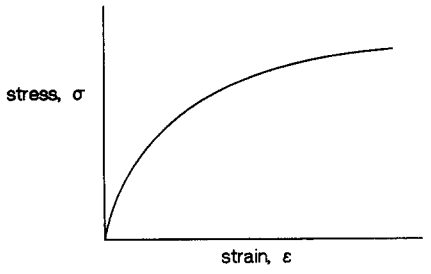

Figure 1 Diagrammatic representation of a stress–strain curve which does not show a local maximum at the yield point

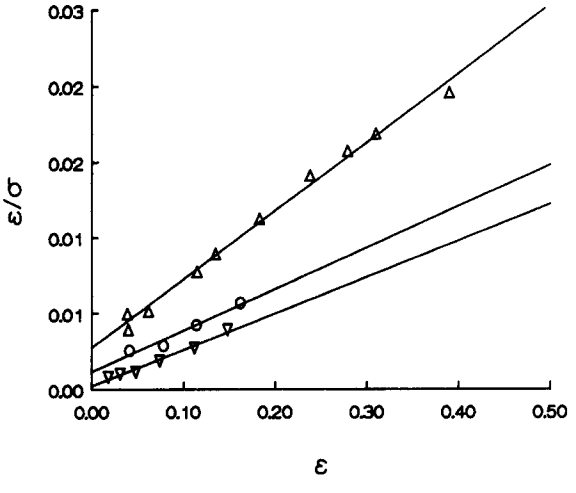

Figure 2 Example of some typical straight lines obtained for ε/σ *versus* ε for the three quenched materials in tension: (△) material A; (○) material B; (▽) material C. These were carried out at 0°C and with a strain rate, $\dot{\varepsilon} = 10^{-3}\ s^{-1}$

σ_c, such that:

$$\sigma_c = \frac{E\varepsilon}{\beta\varepsilon} = \frac{E}{\beta}$$

Combining equation (1) with the Considère construction for a maximum on the force–elongation curve:

$$\frac{d\sigma}{d\varepsilon} = \frac{\sigma}{1+\varepsilon} \tag{2}$$

enables us to predict the strain and stress at which a sample in tension will yield:

$$\varepsilon_{max} = \frac{1}{\sqrt{\beta}} \tag{3}$$

and, the stress at this point

$$\sigma_{max} = \frac{\sigma_c}{1+\varepsilon_{max}} = \frac{E}{\beta+\sqrt{\beta}} \tag{4}$$

So if values for E and β can be determined, the yield stress and strain can be predicted using equations (3) and (4).

By rearranging (1) a linear equation can be obtained

$$\frac{\varepsilon}{\sigma} = \frac{1}{E} + \frac{\beta\varepsilon}{E} \tag{5}$$

This suggests that plotting ε/σ against ε allows values for E and β to be obtained from the intercept and the slope of the line if the time-dependent parameter β remains constant over the strain range. The straight line graphs obtained for a selection of materials are shown in *Figure 2*. The graphs show that for a wide range of strains, where appropriate up to the force maximum, all three materials show excellent straight line fits. At larger strains, deviations from the predicted straight lines occur. These can be due either to necking, preventing the calculation of true stress–strain curves, or to strain hardening due to molecular orientation – which is not modelled by equation (1). These straight line graphs enable values of E and β to be found for each material over a range of conditions. Using these values we can predict an engineering yield point for the materials from the deviations of the stress–strain curve from linear elastic behaviour.

The results showing the yield stress over a range of temperatures for the three materials, obtained from the straight-line analysis, are shown in *Figure 3*, compared with conventional yield points where available. These three polyethylene samples exhibit very different yield behaviours and show markedly different stress–strain curves. Considering this, the values obtained for the yield point were in very good agreement with conventional yield point measurements. The results shown in *Figure 3* provide good justification for using the Brereton analysis to predict yield.

A paradoxical situation is met when we try to combine the Brereton equation (which models a true stress–strain curve with only one maximum at infinite strain) and the Considère condition, which is only met if there is a local force maximum at the yield point. This paradox can be resolved by considering the fact that the Brereton analysis is only applied to the initial strain region where the materials act as non-linear viscoelastic material. The predicted maximum falls outside of this region; although the Brereton analysis smoothly models the curves up to the yield point and indeed predicts it, it cannot model the behaviour at higher strains. In the higher strain regions the material may strain soften, and thus show a maximum in stress, or strain harden so that no maximum is seen, as is explained graphically in *Figure 4*.

We are now in a position where we can measure the yield point but we have to ask the obvious question, what is yield? The conventional yield point, that is the maximum of the force–elongation curve, is the point at

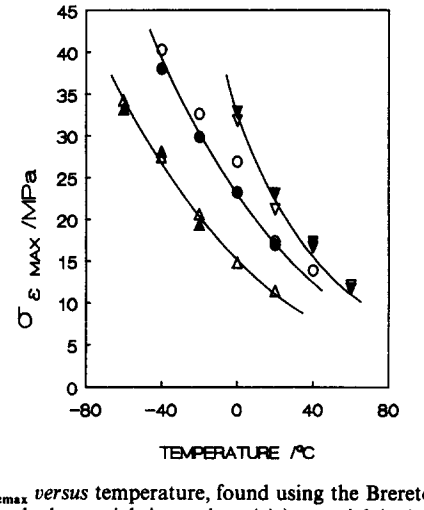

Figure 3 σ_{emax} *versus* temperature, found using the Brereton analysis for three quenched materials in tension: (△) material A; (○) material B; (▽) material C. These are compared with the conventional yield points: (▲) material A; (●) material B; (▼) material C. Strain rate, $\dot{\varepsilon} = 10^{-3}\ s^{-1}$

which the applied strain rate is equal to the plastic strain rate. The onset of necking in the materials is also accepted as a measure of the yield point. A further definition of yield is the point at which permanent deformation occurs. These give us three possible ways of measuring the yield point. Are these three points the same and inextricably linked at the 'yield point'?

The work published by Seguela and Rietsch[2] for polyethylene under tensile loading demonstrated clearly the existence of double yield points for the materials tested. This obviously complicates the measurement of 'a yield point' and, to a degree, the idea of a single measurable yield point for our materials becomes redundant. The work described in this paper is aimed at measuring and characterizing the two yield points. This has enabled us to measure quantitatively these yield points and gain an understanding of the deformation mechanisms involved.

Measurements of the residual strain in compression were carried out to identify yield points and their recovery characteristics. The tests were carried out in compression rather than in tension so that the effects of necking in tension could be overcome. These results themselves are intended to demonstrate the existence of the two yield points, rather than to predict them quantitatively.

The double yield phenomena suggested two processes acting in parallel for these materials and so an attempt was made to try and separate the stress–strain curves for these processes individually using the transient dip tests described by Fotheringham and Cherry[3]. These experiments, their results and the possible implications are described below.

The evidence would seem to indicate that yield in polymers, and for polyethylene in particular, is far more complicated than for an elastic or elastic–plastic material. In some polymers permanent plastic deformation is shown before the conventional yield point and, in others, total recovery is seen past the conventional yield point.

The research we have carried out into the three polyethylene materials has revealed some interesting results and has shown that we must reassess our understanding of yield for polyethylene.

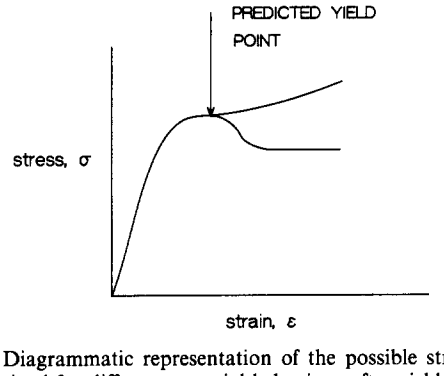

Figure 4 Diagrammatic representation of the possible stress–strain curves obtained for different material behaviour after yield

MATERIALS

The three grades of polyethylene which differ markedly in their chemical structure were obtained from BP Chemicals Ltd. The details of these polymers are given in *Table 1*.

The materials for tensile tests were compression moulded into 0.5 mm thick sheets at 160°C and 138 kPa. These sheets were either quenched in water at room temperature or slow cooled at ~2°C min^{-1} to room temperature. The compression moulded sheets were compressed using a semi-positive technique to give ~12 mm thick sheets. These were also cooled at ~2°C min^{-1}.

RESIDUAL STRAIN EXPERIMENTS

Experimental

Considering our definition of yield as the point at which permanent deformation occurs, it was decided to measure the residual strain as a function of the applied strain. To avoid the problem of necking these tests were done in compression on cylindrical samples (12 mm long, 6 mm diameter). These tests were carried out at 20°C at a strain rate of 10^{-2} s^{-1}. The maximum applied strain was 0.60 and the samples were subjected to applied strains in multiples of 0.06. The residual strain of the samples was measured after 3 days at room temperature.

Results

The residual strain values are shown as a function of the applied strain values in *Figure 5*.

Discussion

The tests have provided some surprising results. For a conventional elastic–plastic solid we would expect a graph with zero gradient for strains below the yield strain, where the samples show total recovery, and then a gradient of unity above the yield strain where there is no recovery of the plastic strain beyond the yield point.

However, our graphs show three different gradient regions. The initial region is for strains up to 5–10% depending on the material where we see total recovery within 3 days. Then we see a second region which has

Table 1 Details of the polymers used

Polymer[a]		$\bar{M}_w$	$\bar{M}_n$	Branch content (10^3 C atoms)	Density (kg m^{-3})	MFI[b]
Material A	Q	126000	30300	21.0 Butyls	917.3	0.9
	SC				922.2	
Material B	Q	206000	12900	6.2 Butyls	932.3	0.2
	SC				940.6	
Material C	Q	131000	19100	<0.1 Butyls	956.0	0.6
	SC				968.0	

[a]Material A is a linear low density polyethylene, material B is a medium density copolymer and material C is a linear high density polyethylene
[b]MFI, melt flow index

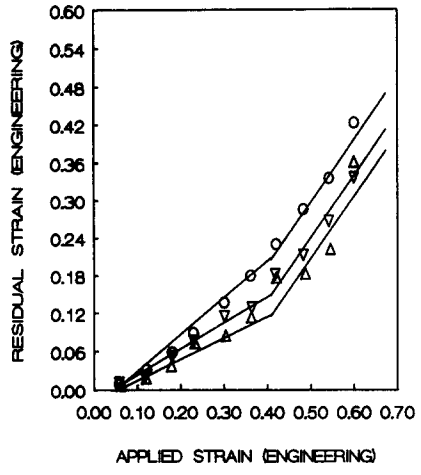

Figure 5 Residual strain–applied strain curves for the three materials in compression: (△) material A; (▽) material B; (○) material C. Strain rate, $\dot{\varepsilon} = 10^{-2}\,s^{-1}$

gradient between 0 and 1, which shows that in this range of strains (10–35%), the material partially recover. Finally we see a region of unity gradient for applied strains above 35%, where the residual strain after 3 days increases directly with the applied strain. This behaviour is exhibited by all three materials. The only difference between the materials is that the most highly branched material showed the most recovery in the intermediate gradient range and the least recovery is shown by the high density material.

These results seem to indicate two yield points associated with the two points on the graph where the gradient changes occur, appearing at approximately the same strains for each of the materials. The first yield point appears to mark the onset of 'temporary' plastic strain. It has to be remembered that the residual strain was measured after an arbitrary period of 3 days at room temperature. It is intended to measure the residual strain as a function of the recovery time and to extend this to a much longer time period, so that the time dependence of the recovery processes can be measured.

In the modelling to be described the first yield is considered to be caused by a dashpot yielding. Permanent deformation is prevented by a spring which acts in parallel with the dashpot and which drives it back when the external stress is removed. The second yield point at ~35% is associated with the onset of totally irrecoverable plastic deformation.

Following the work carried out by Seguela and Rietsch[2] it was decided to carry out similar work on our materials to find whether we could also observe double yield points on the tensile stress–strain curves and to identify these with the two yield points described above. This work is explained in the next section.

DOUBLE YIELD EXPERIMENTS

Experimental

The search for double yield points in our materials was carried out on both the quenched and slow-cooled materials over a range of temperatures at a strain rate of $10^{-2}\,s^{-1}$. These were carried out in tension on dumb-bell shaped samples having an effective length of ~3.4 cm. Photographs of the samples were taken under load to gain an understanding of the deformation and neck formation.

Results

The results of the tensile tests are shown in *Figures 6, 7* and *8* which show the stress–strain relationships for all three quenched materials over a range of temperature. The true stress was calculated assuming a homogeneous strain at constant volume. The photographs showing the deformation of the samples are shown in *Figures 9, 10*

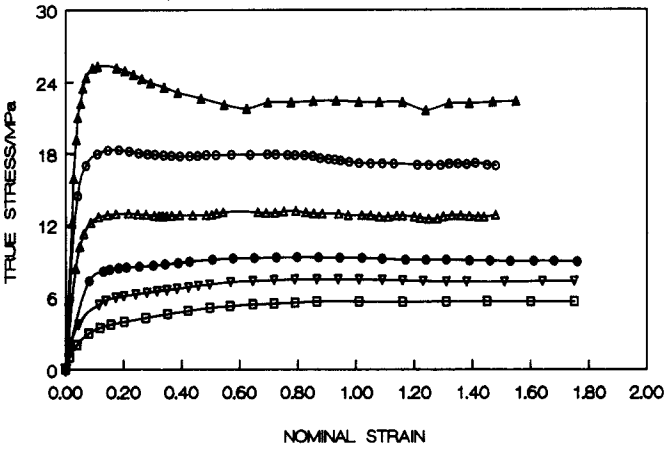

Figure 6 True stress–nominal strain curves for material A 160°C/Q in tension over a range of temperatures (°C): (▲) −40; (○) −20; (△) 0; (●) 20; (▽) 40; (□) 60. Strain rate, $\dot{\varepsilon} = 10^{-2}\,s^{-1}$

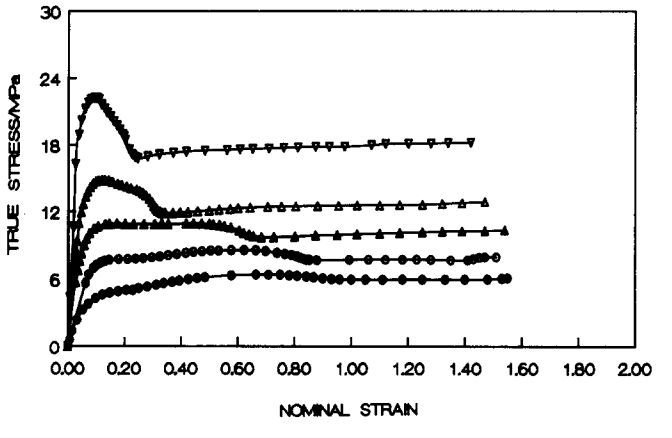

Figure 7 True stress–nominal strain curves for material B 160°C/Q in tension over a range of temperatures (°C): (▽) 0; (△) 20; (▲) 40; (○) 60; (●) 80. Strain rate, $\dot{\varepsilon} = 10^{-2}\,s^{-1}$

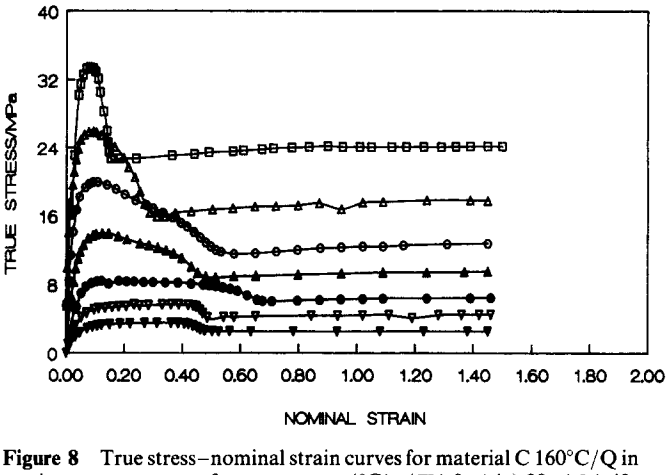

Figure 8 True stress–nominal strain curves for material C 160°C/Q in tension over a range of temperatures (°C): (□) 0; (△) 20; (○) 40; (▲) 60; (●) 80; (▽) 100; (▼) 120. Strain rate = $10^{-2}\,s^{-1}$

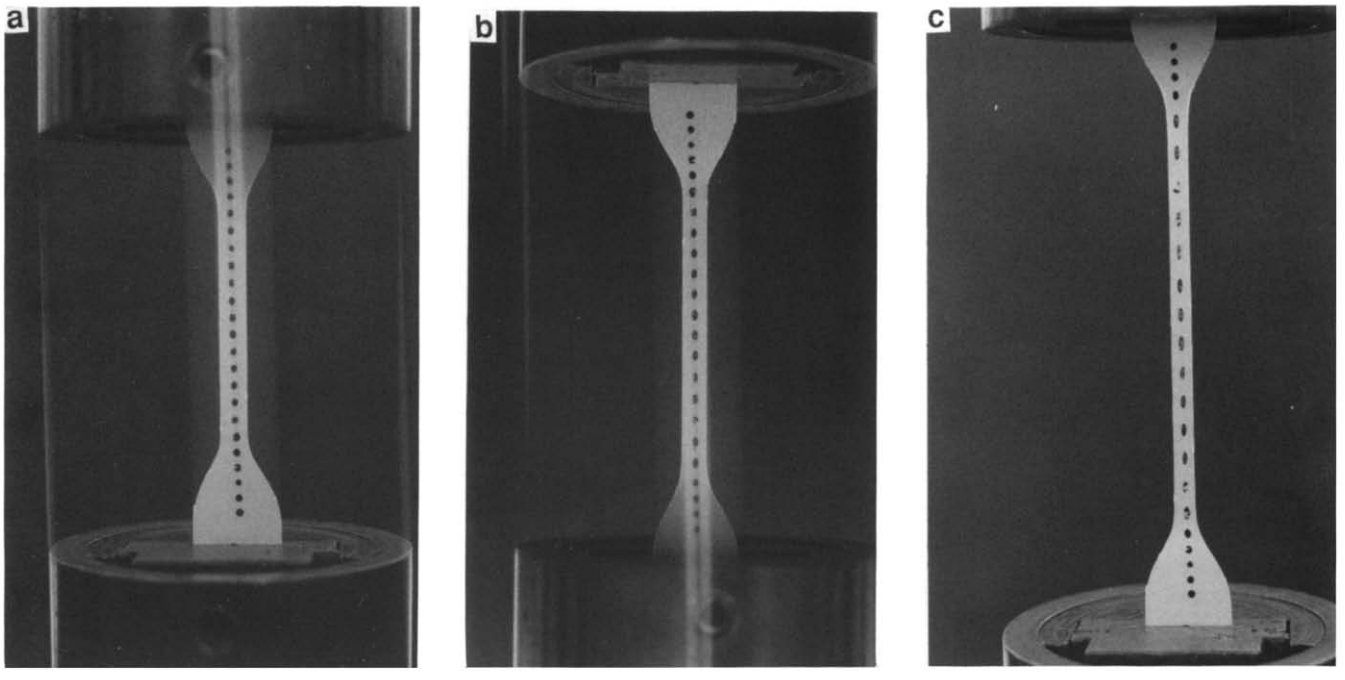

Figure 9 Material A 160°C/Q in tension at 20°C, $\dot{\varepsilon} = 10^{-3}\,s^{-1}$: (a) before first yield point, $\varepsilon = 0.18$; (b) just before second yield point, $\varepsilon = 0.40$; (c) after second yield point, $\varepsilon = 0.96$

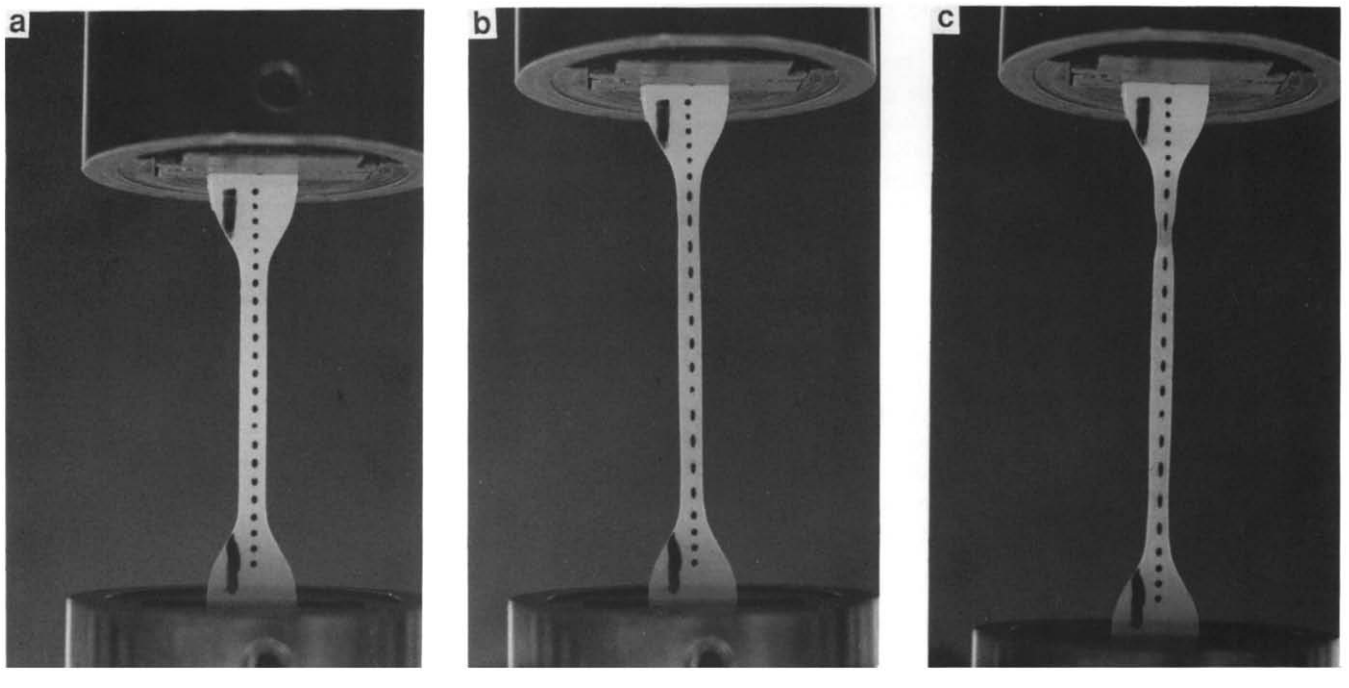

Figure 10 Material B 160°C/Q in tension at 20°C, $\dot{\varepsilon} = 10^{-3}\,s^{-1}$: (a) before first yield point, $\varepsilon = 0.22$; (b) just before second yield point, $\varepsilon = 0.59$; (c) after second yield point, $\varepsilon = 0.77$

and *11*. The three photographs show the samples before the first yield point, and just before and after the second yield point.

Discussion

The stress–strain curves for all three materials clearly show the existence of double yield points in all three of these materials. At low temperatures a sharp first yield point is seen, but as the temperature increases, this gradually becomes less pronounced and a broader second yield process seems to dominate at higher temperatures.

Photography of the samples showed that the first yield point is associated either with no neck or with only a very shallow neck in the samples. The first yield point seems to be associated with an intrinsic strain softening process within the materials which is more pronounced at low temperatures. The residual strain results show that this first yield is either partially or totally recoverable given favourable conditions. A sharp neck is only seen at the second yield point. It is the second yield point which is related to permanent deformation in the samples and is associated with sharp necking, so it can be concluded

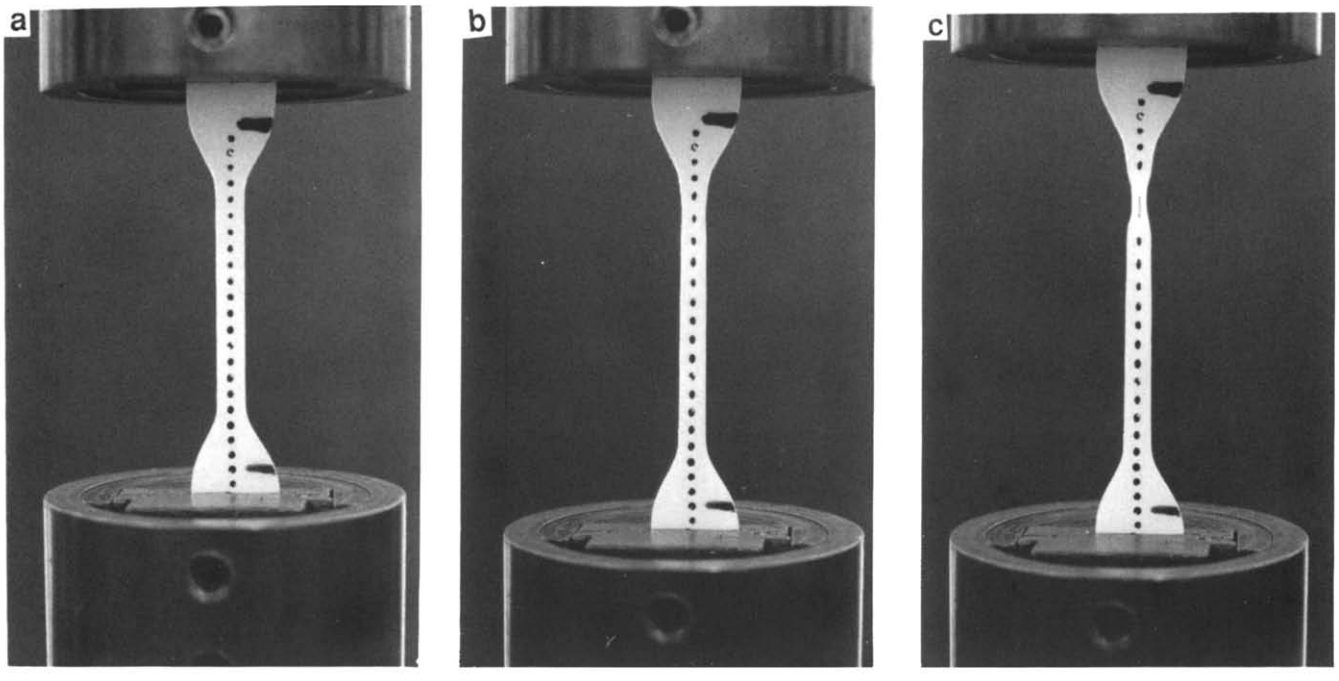

Figure 11 Material C 160°C/Q in tension at 20°C, $\dot{\varepsilon} = 10^{-3}\ s^{-1}$: (a) before first yield point, $\varepsilon = 0.13$; (b) just before second yield point, $\varepsilon = 0.31$; (c) after second yield point, $\varepsilon = 0.46$

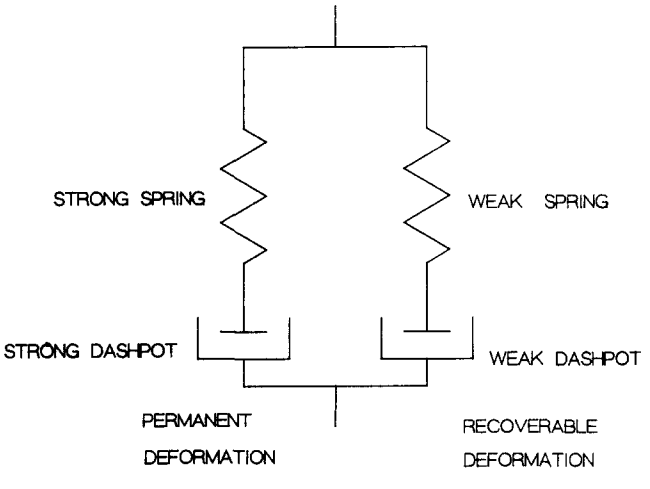

Figure 12 Ward and Wilding model[4] used to describe creep behaviour of melt spun high modulus polyethylene fibres

that this yield is associated with a more drastic breakdown in the structure of the polyethylene.

The double yield may be interpreted mechanically as the individual yield of two highly non-linear dashpots arranged in parallel as shown in *Figure 12*. The evidence would suggest that over the range of conditions covered here the first yield point is associated with a 'weak' dashpot which has a strong spring in parallel with it. Recovery is caused by the strong spring 'driving back' the weak dashpot when the external stress is removed. Conversely the second yield point is associated with a 'strong' dashpot which is in series with the strong spring and yields only at high stresses.

The evidence suggests that we can model the yield behaviour of these materials using two non-linear Maxwell elements in parallel. This model has also previously been used by Wilding and Ward[4] to describe the creep behaviour of melt spun high modulus polyethylene fibres. Although the structures of the isotropic materials studied here differ significantly from the ultra-high modulus materials, surprisingly it does appear that they may be modelled in the same way. The Wilding and Ward work suggested that one dashpot has a comparatively small activation volume, which could possibly be associated with a slip process in the crystalline region. The second dashpot has a comparatively large activation volume and is possibly associated with a semicrystalline or amorphous region. Preliminary investigations into our materials has confirmed these findings.

It is clearly important to try and separate the two arms and so obtain the stress–strain curves for each arm to give a better understanding of the physical processes involved at the yield points. The method used is explained in the next section together with the results obtained.

TRANSIENT DIP EXPERIMENTS

Experimental

The experimental technique used was based on the transient dip experiments described by Fotheringham and Cherry[3]. Tests were carried out in both compression and tension. The tensile tests were carried out on both quenched and slow-cooled materials at three strain rates (10^{-2}, 10^{-3} and $10^{-4}\ s^{-1}$). It was found that accurate recovery stress data were very difficult to obtain at strain rates above $10^{-3}\ s^{-1}$ and so were prone to large errors. The strain was taken as the engineering strain and the true stress was calculated assuming deformation at constant volume.

The first step is to simplify the model developed in the previous section. The model is modified by replacing the weak arm with a single dashpot and the strong arm with a single spring (*Figure 13*). This is similar to the Haward and Thackray model[5] used by Fotheringham and Cherry[3]. The spring is associated with the process of

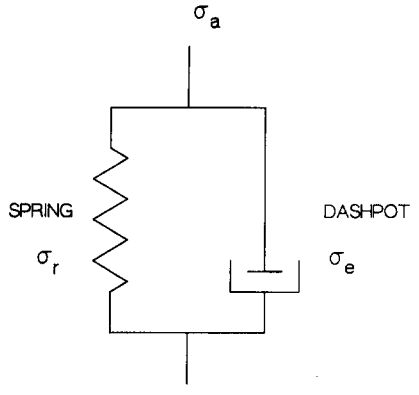

Figure 13 Howard and Thackray model used to describe the mechanical behaviour of material subjected to the transient dip test

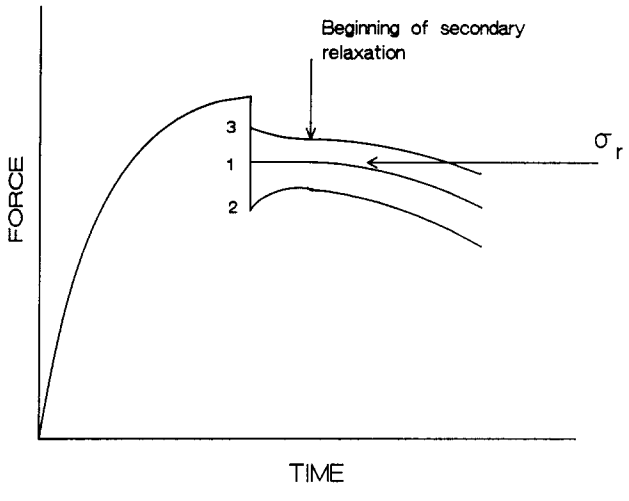

Figure 14 Diagrammatic representation of possible force–time curves seen for the transient dip tests (see text)

recovery and is responsible for the recovery stress, σ_r.

The effective stress on the dashpot is σ_e. If we apply an external stress σ_a then σ_e is given by:

$$\sigma_e = \sigma_a - \sigma_r$$

If we have a situation where the applied stress is equal to the recovery stress then the effective stress on the dashpot is zero and so will be the strain rate in the dashpot. This will allow us to determine the recovery stress.

The transient dip experiment involves a rapid unloading step from a point on the stress–strain curve to a new test stress, σ_T. By holding the strain constant at this point the reaction of the stress can be found as a function of time. Three possible situations can occur:

1. $\sigma_T = \sigma_r$; strain rate in the dashpot is zero and the stress initially remains constant as a function of time.
2. $\sigma_T < \sigma_r$; σ_e is negative and relaxes to zero causing the applied stress to increase with time.
3. $\sigma_T > \sigma_r$; σ_e is positive leading to relaxation of stress with time.

These three possible situations are shown graphically in *Figure 14*. Both σ_e and σ_r can therefore be found as a function of the applied strain.

Results

The values of σ_r and σ_e against strain are shown for material A 160°C/Q in tension over a range of temperatures are shown in *Figures 15* and *16*. Of the three materials material A 160°C/Q shows the most homogeneous deformation and so the values of true stress are most reliable for this material. Similar results were obtained for the two other materials in both tension and in compression.

The results obtained for material A for σ_r, σ_e and σ_a were analysed using the Brereton analysis to find the yield points for the applied stress and the two arms separately. The results are shown in *Figures 17* and *18*.

Discussion

The results obtained for the transient dip experiments have been very encouraging. The stress–strain curves obtained have shown that over the entire range of temperatures and strains used that $\sigma_r \gg \sigma_e$. The error associated with σ_r is also much smaller than that for σ_e and these results are considered more reliable as a result.

The predicted yield points for the two arms individually showed that the weak arm yields at a lower strain than the strong arm, giving further evidence for the existence of two individual yield points.

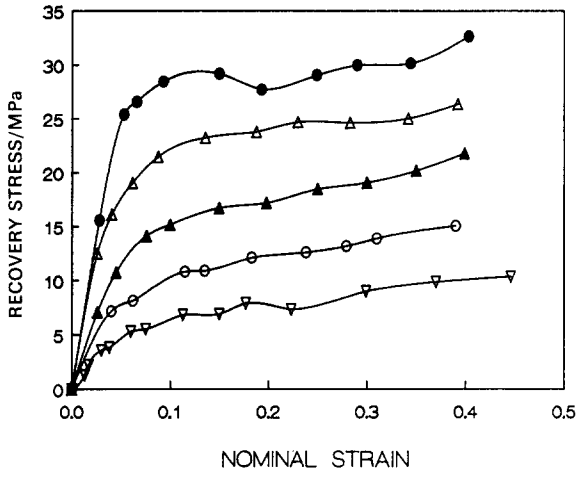

Figure 15 Recovery stress–nominal strain curves for material A 160°C/Q over a range of temperatures (°C): (▽) 20; (○) 0; (▲) −20; (△) −40; (●) −60. Strain rate, $\dot{\varepsilon} = 10^{-3}\,s^{-1}$

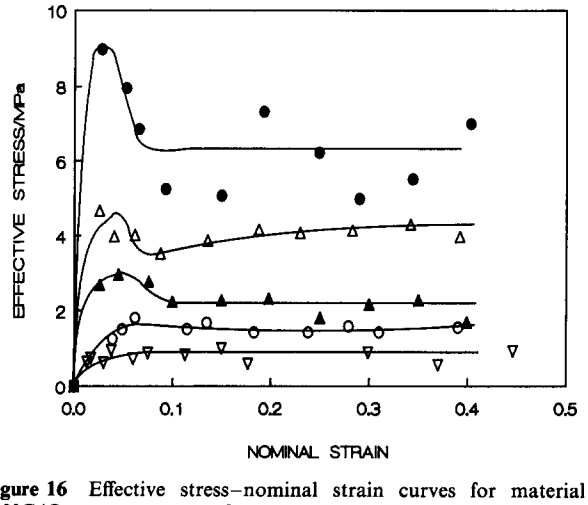

Figure 16 Effective stress–nominal strain curves for material A 160°C/Q over a range a of temperatures (°C): (▽) 20; (○) 0; (▲) −20; (△) −40; (●) −60. Strain rate, $\dot{\varepsilon} = 10^{-3}\,s^{-1}$. Curves drawn by hand

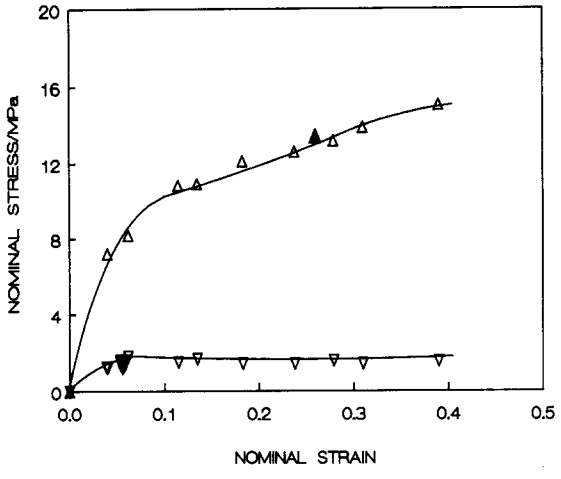

Figure 17 Nominal stress–nominal strain curves for material A 160°C/Q at 0°C and with a strain rate, $\dot{\varepsilon} = 10^{-3}\,s^{-1}$. The predicted yield points for recovery stress, σ_r (△) and effective stress, σ_e (▽) from Brereton analysis are also shown: (▲) σ_r yield; (▼) σ_e yield

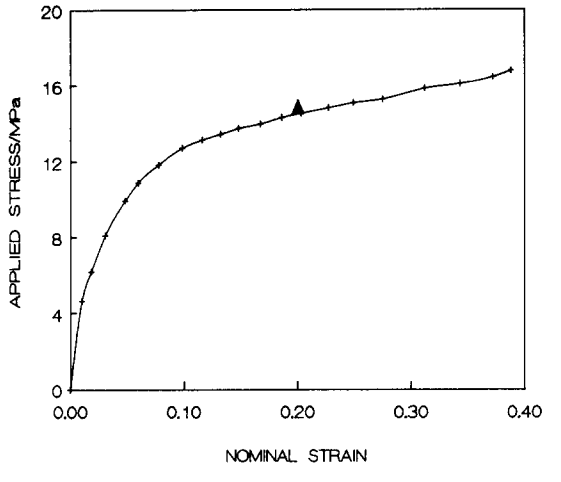

Figure 18 Applied stress–nominal strain curve for material A 160°C/Q at 0°C and with a strain rate, $\dot{\varepsilon} = 10^{-3}\,s^{-1}$ showing the yield point (▲) predicted by Brereton analysis

GENERAL DISCUSSION

The work carried out so far has identified some fundamental questions as to what we understand by yield in polyethylene. Based on the work carried out by Seguela and Rietsch[2], the mechanical work has been aimed at demonstrating the existence of double yield points in our material, and then further to characterize these points. We have been able to draw some conclusions as to the mechanical behaviour of the two processes from the experimental findings of both the residual strain and transient dip experiments.

Our findings show the first yield point is associated with low stress and strain values. It is not associated with necking and is either partially or totally recoverable. The second yield point occurs at higher stress and strain values; it is associated with necking of the material and is irrecoverable. A local maximum in the force–elongation curve may be associated with either of the yield points: at the first yield point this is intrinsic, and due to a strain-softening process, whereas a load maximum at the second yield point is geometric, and due to the necking of the materials.

The work carried out has enabled us to identify two extreme types of curve (A and B) as shown schematically in *Figures 19* and *20*.

The type A curve is typically seen at low temperatures and high strain rates, where the shape of the stress–strain curve describing the first yield process is the major factor in determining the shape of the applied stress curve. The shape of the stress–strain curve describing the second yield point is effectively hidden at the first yield point because it is changing only slowly with strain in this range. Applying the Brereton analysis to this type of curve predicts the first yield point.

The type B curve is typically seen at high temperatures and low strain rates where the contribution of the first yield process is less pronounced because it is relatively small and varying only slowly with strain; the shape of the second yield process becomes dominant and so the Brereton analysis predicts the second yield point for this type of curve.

In between the two extremes there is an area where no one process dominates and the Brereton analysis becomes less reliable. The major problem with using the Brereton analysis for the total stress–strain curves is that we are dealing with the sum of two individual curves which may have very different forms. For the individual stress–strain curves for both arms obtained from the transient dip tests the Brereton analysis gives generally good results and can easily be justified in terms of the Considère yield point.

The Brereton analysis therefore gives us a method of measuring the 'yield' of our samples from the initial strain region. Because the materials differ in their behaviour once the dashpots start to yield, either strain hardening or strain softening, the Brereton yield point may not be associated with a physical point on the force–elongation curve, i.e. a local maximum. The modelling of the initial strain region predicts a maximum in the nominal stress which may not, in fact, be observed because of the intervention of other mechanisms. The Brereton analysis

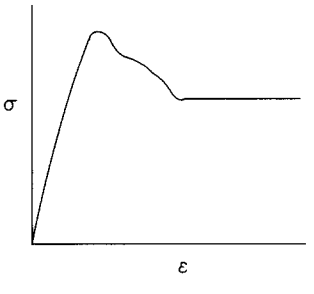

Figure 19 Diagrammatic representation of a typical type A stress–strain curve seen at low temperatures and high strain rates

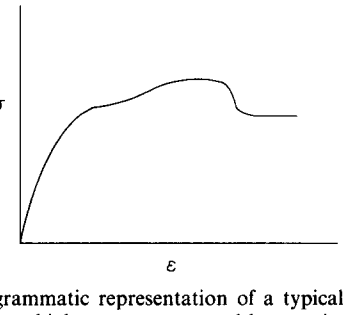

Figure 20 Diagrammatic representation of a typical type B stress–strain curve seen at high temperatures and low strain rates

gives us a justfiable way of measuring yield for the two individual arms and can also be used for the total applied stress to find a quantitative engineering parameter which may or may not be related to the onset of permanent deformation or necking.

CONCLUSIONS

The work described has shown evidence to support the concept of a double yield process in polyethylene. Double yield points are evident from the tensile stress–strain curves obtained for our three materials over a range of temperatures and from the residual strain experiments in compression. Photography of the tensile samples shows that necking is associated with the second yield point.

The two yield points are modelled by two non-linear Maxwell elements in parallel. Using the Fotheringham and Cherry transient dip techniques these two arms can be separated to give the stress–strain curves of the two arms individually.

By mathematically modelling the stress–strain curves, and combining this model with the Considère construction, predictions can be made for the point at which necking begins, i.e. the conventional yield point. The results obtained from this analysis are consistent with those for conventional yield points.

ACKNOWLEDGEMENTS

Thanks are due to BP Chemicals Ltd, Grangemouth for providing the materials and financial and technical support for the project under the SERC 'CASE' Programme. Special thanks go to Mr A. D. Channell, Dr M. J. Cawood and Dr A. Gray for their contributions.

REFERENCES

1 Brereton, M. G., Croll, S. G., Duckett, R. A. and Ward, I. M. *J. Mech. Phys. Solids* 1974, **22**, 97
2 Seguela, R. and Rietsch, F. *J. Mater. Sci. Lett.* 1990, **4**, 46
3 Fotheringham, D. G. and Cherry, B. W. *J. Mater. Sci.* 1978, **13**, 951
4 Wilding, M. A. and Ward, I. M. *Polymer* 1981, **22**, 870
5 Haward, R. N. and Thackray, G. *Proc. R. Soc.* 1968, **A302**, 453